Proceedings of the 3rd International Conference on Materials Chemistry and Environmental Engineering (CONF-MCEE 2023), Part II
DOI: 10.54254/2755-2721/7/20230409

A review of bio-inspired fouling resistance surfaces

Sanchuan Che[1+,7], Muyi Ye[2+], Kayiu Li[3+], Yang Xie[4+], Pengyou Du[5+], Hunan Deng[6]

[1]Department of Chemical and Environmental Engineering, University of Nottingham, Nottingham, NG7 2JG, United Kingdom
[2]Department of Biochemistry, Case Western Reserve University, Cleveland,44106, The United States
[3]Hangzhou Foreign Languages School, Cambridge A-Level Centre, Hangzhou,310023, China
[4]Cambridge International Centre of Tung Wah High School, Dong guan,523000, China
[5]International Department, Shanghai World Foreign Language Academy, Shanghai,200233, China
[6]Shanghai Weiyu International School, Shanghai,200231, China
+These authors contributed equally to this work and should be considered co-first authors

[7]Chesanchuan@126.com

Abstract. Solid fouling settlement, defined as the unexpected payment of various types of solid contaminants, including ice, wax, bacteria, and protein, can result in many problems in daily life and production and cause economic and security losses. Despite many traditional methods for reducing foulant to make a more durable and efficient antifouling surface, many artificial surfaces inspired by the natural antifouling material which the environment has selected during the process of evolution, including lotus leaf, pilot whale skin, gecko feet, shark skin, and pitcher plant are developed to resist adhesion of multiple foulants in an efficient and environmentally friendly way. In this review, the mechanism of how surfaces using patterns similar to the natural antifouling surface resist fouling materials is overviewed. Various methods for fouling formation classify the hazard, properties, and characteristics of different fouling materials. The approaches typically applied in designing a surface with high fouling resistance are presented first. After interpreting the theories and models mentioned in the explanation of the fouling resistance property, the textural microstructures, the chemical and physical properties used, and applications for fouling resistance of several bio-inspired fouling resistance surfaces, and how these surfaces can be improved in the future are discussed.

Keywords: Bio-inspired, fouling resistance, superhydrophobic.

DOI: 10.54254/2755-2721/7/20230409

1. Introduction

1.1. Background of fouling

1.1.1. Definition of fouling. "Fouling is the settlement of unwanted materials on solid surfaces. It usually reduces the performance of the affected surface. Foulants consist of either living organisms or non-living substances." [1] Fouling can cause various detrimental effects on the impacted surfaces. Those effects include reducing the efficiency of a machine or membrane, additional drag to the boat, shortening the surface's lifespan, and so on.

1.1.2. Fouling classification. Fouling materials have many types, most of which can be put into two groups, soft fouling materials, and hard fouling materials. The method to divide them is using the concept of Young's modulus, which measures a solid material's tensile or compressive stiffness. It's the value of the stress to the axial strain when force is applied to the material.

To be more specific, we can put different fouling into five more detailed classifications.

a) Particulate fouling

Particulate fouling is the accumulation of solid particles suspended onto a surface. The fouling starts with the deposition of small particles on a clean surface; then, this process will keep occurring to the level that all the cross-section area is wholly blocked, which affects the normal working conditions.

b) Chemical reaction fouling

Chemical reaction fouling is the deposition formed by the chemical reaction, but the surface material does not participate in the response. The formation of chemical fouling generally has three processes; at first, reactants will react, and they form precursors which are soluble in the fluid, then the precursors form the deposit by the reaction on the wall. Polymerization, cracking, and coking of hydrocarbons are all examples of reaction fouling. The formation rate of fouling is mainly affected by the factor of temperature, and the composition of the fluid or gas past the surfaces also affects the reaction fouling.

c) Corrosion fouling

Corrosion fouling is the deposit of the corrosion products of the surfaces; most metal surfaces can be affected by this fouling. The corrosion of surfaces is considered to be affected by two factors, oxygen, and water. The metal surfaces exposed to open air and can contact with water will be eroded and converted to more chemically stable oxide.

d) Precipitation fouling

This fouling mostly takes place on surfaces with prolonged contact with water; soluble salts, oxides, and other chemicals precipitate on the wall when they reach saturation in the water solution; also, when their solubility changes with temperature, they may crystallize on the surfaces of the container of the solution.

e) Biological fouling

Biological fouling consists of microorganisms (i.e., Bacteria, fungi, algae), other living plants, and small animals. They are often found on the bottom of the ship, pipework underwater, and in ponds. Some biological fouling would lead to corrosion of the surfaces they attached to, affecting the device's normal function. The biofilm on medical devices has led to severe healthcare problems. They are the accumulation of micro-organisms and are closely related to infectious diseases like dental plaque, upper respiratory infections, peritonitis, urogenital infections, and conditions associated with medical devices, including a total artificial heart. [2] Marine fouling is a particular class in all of the foulants. Marine fouling is the accumulation of different species of marine animals and plants. Those animals and plants form a whole community on the fouling.

f) Solidification fouling

The solid fouling deposit forms when liquid "freezes" onto the surfaces. For example, ice forms on walls in winter. This kind of fouling needs a condition that is cold enough for the fluid to freeze and

DOI: 10.54254/2755-2721/7/20230409

stack on the surfaces. Ice fouling is the accumulation of freezing ice on surfaces. Ice fouling puts severe challenges on the covers of mechanical devices. Like the airplane wings and power lines, as well as locks. Another industry, like renewable energy, is also impacted. Ice fouling impedes the function of solar panels and wind turbines. [3]

1.1.3. Traditional methods to reduce fouling. Many traditional methods to reduce fouling have been developed to resist various foulants with different chemical compositions, microstructures, and physical properties [3]. Standard treatments include coating the surface with polymers, using chemicals repressing the settlement of fouling, like toxic antifouling coatings, to avoid the colonization of sessile marine life, including barnacles or mussels, on the ship[4], and physical cleaning and disinfecting[5]. Most of these methods are non-persistent and inefficient. The limitation of those traditional methods leads to the motivation for developing novel antifouling surfaces, and many characters have indeed been designed over the last three decades to resist the adhesion of fouling materials[3]. These surfaces usually imitate the optimum structure design of the natural antifouling characters like pitcher plant and shark skin which have adapted to their environment in the process of evolution, so that the surfaces with similar structures can be antifouling as well as more environmental-friendly[6]. However, many of those surfaces can address the settlement of only one type of foulant, which limits the application of these surfaces[3]. For example, many conventional antifouling coatings would still be attached by some diatom species like Amphora and Navicula[7]. Thus, significant research has been done to establish a methodology for designing antifouling surfaces that can resist multiple fouls simultaneously [3].

1.2. Design strategies

Before discussing specific design strategies, it is essential to clarify that the antifouling ability has little to do with surface hydrophobicity. For example, the artificial surfaces inspired by both lotus leaf and shark skin have strong hydrophobicity. They are resistant to much organic fouling but do not resist other kinds of fouling, like ice[8].

Different from designing a hydrophobic surface, the antifouling surface designing approaches can usually be classified into three categories. The first strategy to control surface chemistry aims to reduce the substrate's surface energy or to lead the interaction between the foulants and the surface in a specific way[3]. The surface energy is the energy required to break intermolecular force, mainly Van der Waals force, for creating a new surface[9], and the adhesion between fouling materials and texture, called the work of adhesion, would be weaker if the surface energy is lowered. The relationship between the work of adhesion and the interfacial free energy of a surface (γ_{s_1v}) would be illustrated by the equation $\mathrm{Wa} = \gamma_{s_1v} + \gamma_{s_2v} - \gamma_{s_1s_2}$, and the γ_{s_2v} and $\gamma_{s_1s_2}$ are the interfacial free energy for fouling-substrate interface and the fouling[8]. In the case of reducing the surface energy, many modifications, including plasma treatment and polymer blending, would be done[9]. The most common application of this approach is fluorinated polymers like Teflon. Fluorine has strong electronegativity, and the CF bond is polar, so the electrons are harder to move far away from fluorine atoms, and the surface energy would be low. The surface chemistry interacting specifically with the fouling would also function well[8]. Enzymes on the surface could diminish the attachment intensity of barnacles and other organic fouling[4], and the toxic-releasing surface, like Nitric oxide-releasing materials, could release NO adhered to a character or contained in a polymeric delivery agent to kill the bacteria[10,11]. Another common material used for the antifouling surface is a zwitterionic polymer, like P(MMA-co-DMAEMA) blend membrane quaternized by p-chloromethyl styrene (p-CMS) having the double bond introduced, which is usually prepared for antifouling membrane [12].

The second strategy for antifouling surface design is the modification of the microstructure. Although the microstructure is a crucial component for preventing liquid fouling and many fouling with low modulus[3,8], like in the case of resisting solid fouling with high modulus[3,8], the microstructure would be considered detrimental[3-7]. The adhesion of the most common foulants would be increased by the roughness and topography of materials. The area allows the fouling to

DOI: 10.54254/2755-2721/7/20230409

attach increases, enabling protection from hydrodynamic shear forces that can assist in removal [13]. For example, on the rough surface of mild steel, it was estimated 30 times greater settlement of calcite crystal than that of smoother [14]. By the way, the substrate's roughness and the exfoliants' size determine the essentialness of roughness for fouling settlement [7]. As mentioned previously, when the fouling has a high modulus, the surface using this approach would be designed to lower the roughness of the surface so the fouling would be less likely to attach. Taking the SLIPS structure, the structure used by the pitcher plant, as an example, the Slippery Liquid-Infused Porous Surfaces has many porous containing liquid or topography to create the slippery surface so that the fouling would be easily removed and hard to attach [8]. The principle of SLIPS will be shown in the chapter below.

Meanwhile, the surface imitating squid's body also used a similar strategy. In the squid's character, there is a layer of coating in which the hydrophilic segment would be elevated to the coating-seawater interface, so the surface would have a hydration layer formed to prevent the settlement of fouling material[15]. However, some specific surface microstructures can resist certain fouling materials well particularly, like the re-entrant surface reducing the barnacles' underwater attachment[11] and the surface pattern of rice leaf and butterfly wings combining the effect of lotus leaf and shark skin[16].

The final antifouling surface designing strategy is to change the physical characteristics, especially the elastic modulus. For hard fouls settled to the elastic surface, the adhesive strength σ is proportional to the $\sqrt{W_a E/t}$ where E is the elastic modulus and t is how thick the film is[17]. As the elastic force is the force released against deformation, the overall surface energy would be increased when the foulant attaches to the surface, so both the elastic modulus of fouling materials and the surface would affect the adhesive bond strength, so researchers usually classify foulants into hard and soft fouling based on the modulus and dimensions of fouling [16]. A lower elastic modulus is desirable by using this approach to design antifouling surfaces. The reduction in elastic modulus could significantly decrease the adhesion of solid fouling. The modulus between the hard and soft surfaces ranges over five orders of magnitude, so with the deformation happening, the modulus decrease could function more effectively in reducing the strength of the adhesive bond than the inherent surfaces' adhesive strength[18]. For example, as a familiar marine creature with a soft body, a squid's cover with a low elastic modulus (only 0.5–1.0 Mpa elastic modulus for cuttlefish) is rarely adhered by marine foulants, unlike other aquatic animals such as whales and sea turtles, and according to the research comparing the PVP-OH cross-linking PDMS-based polyurethane with lower elastic modulus, which squid inspires, and the un-modified PDMS-based polyurethane coating PVP-0-SiPU, the settlement of fouling organisms on the coating surface significantly reduced[15] (Figure 1).

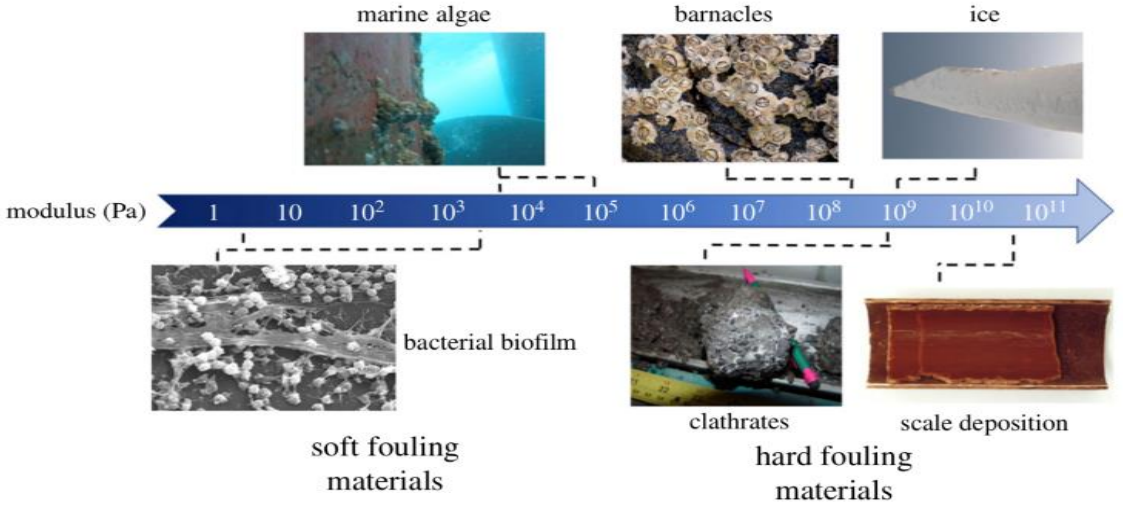

Figure 1 . Different types of fouling materials and their associated moduli, including the soft foulant like biofilm on the catheter and marine algae on a vessel, and the rigid foulant such as barnacles, clathrates in oil pipe, ice attached to the wind turbine vane, and inorganic scale settled in a pipeline.[3]

DOI: 10.54254/2755-2721/7/20230409

2. Basic theories

2.1. Contact angle

A substance's atoms or molecules experience cohesive force with each other. In this case, those on the surface will have fewer atomic neighbors to form cohesive bonds, so they have higher energy than atoms or molecules inside most of the material. The work required per unit area to build a new surface, which correlates to the character's additional power, was typically defined as surface energy. The units of surface energy are J/m^2 or N/m [19]. While contacting with air or any other gas, a liquid droplet tends to contract to resist an external force. As shown in Fig.2, such a tendency is defined as surface tension, γ. γ_{SV}, γ_{LV}, and γ_{SL} are separately the solid-vapor, solid-liquid, and liquid-vapor interfacial tension according to the different contacting surfaces. The surface tension can usually represent the specific Gibbs free energy of the character but not comprise the whole surface energy [20]. A droplet's shape on a flat, solid surface depends on the energy present at the interface between the liquid, reliable, and vapor phases. The contact angle is the angle, θ, formed by surface tension between the liquid-vapor and solid-liquid surface [21] (Figure 2).

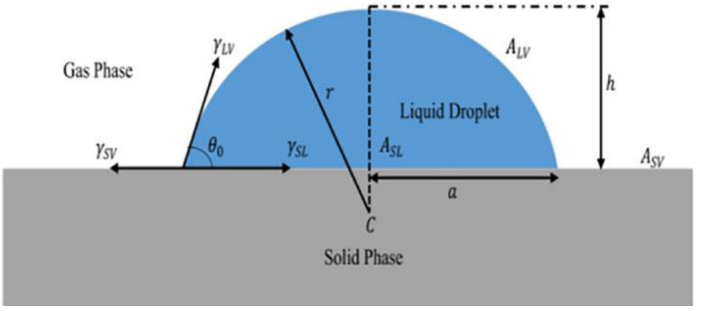

Figure 2. Schematic of the surface tension of a liquid in contact with a solid surface. Image adapted from reference [20].

2.2. Wetting models

Several wetting models were built to calculate contact angle on a surface, including Young's model, Wenzel's model, and Cassie-Baxter's model.(Fig.3) When a drop of liquid comes into contact with a solid, there are three interfaces:liquid-vapor (LV), solid-vapor(SV) solid-liquid(SL), accompanied by three interfacial tensions($\gamma_{SL}, \gamma_{SV}, \gamma_{LV}$). And in1805, Young's equation is developed, which was the earliest model, it is expressed by[21,22]:

$$\gamma_{SV} = \gamma_{SL} + \gamma_{LV} \cos\theta$$

It is worth noting that the force at the horizontal direction should be balanced:

$$F = \gamma_{SV} - \gamma_{SL} - \gamma_{LV} \cos\theta$$

Thus,

$$\cos\theta = \frac{\gamma_{SV} - \gamma_{SL}}{\gamma_{LV}}$$

For a small drop of liquid, under the condition of $(\gamma SV - \gamma SL) > \gamma LV$, which means the surface energy of the interaction between solid and vapor should be more significant than that of solid and liquid, then the drop of liquid will spread($\theta = 0°$). If this condition is not met, the contact angle exists. When $\theta > 90°$, the surface is called hydrophobic; when $\theta < 90°$, the surface is called hydrophilic.[23] The higher the contact angle, the hydrophobicity of the surface increases, and the surface become water-repellent. Nevertheless, this equation is only suitable for the surface under the ideal state, without surface roughness.

DOI: 10.54254/2755-2721/7/20230409

In practice, most surfaces possess some inherent roughness is introduced. Simultaneously, the assumption of the drop of liquid will enter the grooves, where the tracks have chemical homogeneity. [23]In 1936, the Wenzel's model stated the relationship between roughness and contact angle：

$$cos\theta\hat{} * = r\, cos\theta$$

Where θ* represents the apparent contact angle, which is the angle between the tangent of the interface of liquid air and the solid surface, and θ represents Young^'s s contact angle. Wenzel model gives a definition of roughness, r , which is the ratio of actual surface area to its projection area on the plane[24]:

$$r = \frac{\text{Actual surface area}}{\text{projected surface area}}$$

For ideal surfaces, $r = 1$, since all surfaces are rough, $r > 1$ is always true: $\cos\theta^* > \cos\theta$. Under this condition, there are two distinct situations:(1) when θ<90°, θ*is smaller than θ, the surface will become hydrophilic. (2) when θ>90°, θ*is larger than θ, the surface will become hydrophobic.

Hence, the increased roughness leads to an increased contact angle. The liquid-vapor interfacial surface tension will stay constant, although liquid-solid interfacial and solid-vapor interfacial tension increase.[22].

Wenzel's model considers that all pits are homogeneous and completely wet (Fig.4), without air pockets. In contrast, if the liquid does not wet the protrusion thoroughly, then an air pocket exists underneath the liquid droplet [24]. In 1944, the Cassie-Baxter model refined the calculation theory based on Wenzel's model. As mentioned, the roughness becomes larger, and the drop of liquid contact the peak of grooves instead of entering since the surface part is occupied by air. The equation of the Cassie-Baxter model is[24]:

$$\cos\theta^* = f_1\cos\theta_1 + f_2\cos\theta_2$$

$$f_1 + f_2 = 1$$

f_1 and f_2 are the fractions of solid and fraction of air, respectively. Since the air is enclosed in the grooves, the contact angle of liquid with air is 180°, which means θ_2=180°, it leads to the further transformation of the equation:

$$\cos\theta^* = f_1(\cos\theta_1+1)\text{-}1$$

In Cassie-Baxter model, it indicates the relationship between wettability and the surface structure and the chemical composition of the surface. [19]'(Figure 3 and Figure 4).

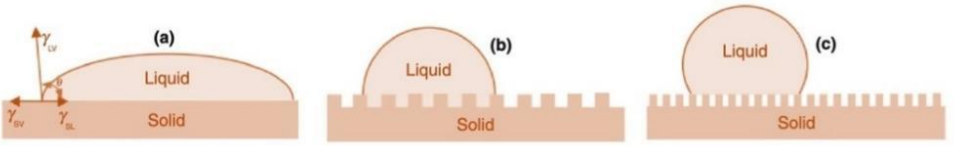

Figure 3. The droplet on superhydrophobic surfaces in different models. (a)young's model. (b)wenzel's model. (c) cassie-baxter's model.[23]

DOI: 10.54254/2755-2721/7/20230409

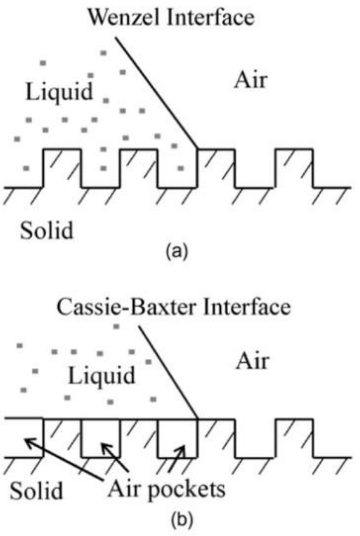

Figure 4. (a) It is at wenzel's model. The pits are symmetrical and completely wet. (b) cassie-baxter equation for the composite interface with air pockets.[19]

2.3. Contact angle hysteresis

Contact angle hysteresis describes the difference between advancing and retreating contact angles. The observed contact angle before the contact line moves forward while the contact angle is growing is known as the advancing contact angle, θ_{adv}. On the other hand, the receding contact angle, θ_{rec}, is the observing contact angle at which the contact line starts to recede when the contact angle decreases [25] (Figure 5).

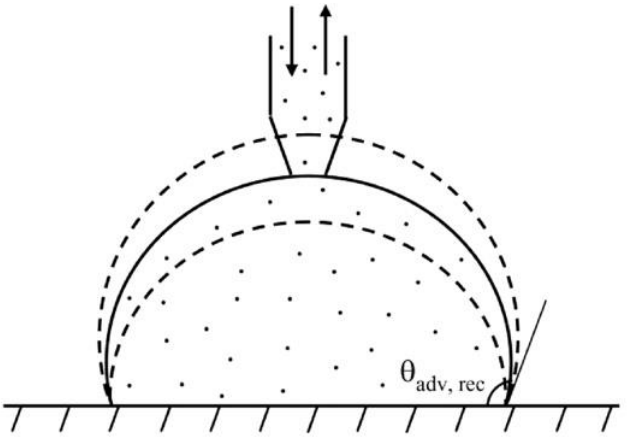

Figure 5. Liquid droplets are added or removed while they contact a rough surface. Image adapted from reference [19].

Contact angle hysteresis could not be entirely removed because of two factors of contact angle hysteresis: heterogeneity and roughness [19]. Generally, while the contact line of a liquid is moving on a heterogeneous surface, its speed is lower than that of a homogeneous surface. That's because of the pinning and depinning events. The other factor is roughness – in reality, most solids are not entirely smooth [25]. As shown in Fig.6, zooming into the microscale, any local slope contributing to the roughness would change the advancing and receding contact angle, altering the contact angle hysteresis (Figure 6).

DOI: 10.54254/2755-2721/7/20230409

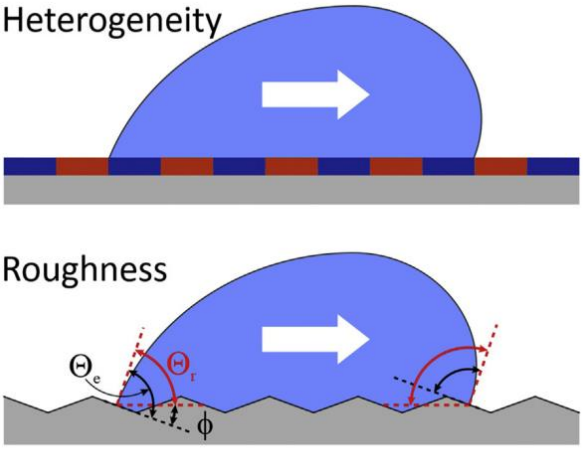

Figure 6. Heterogeneity and roughness contribute to contact angle hysteresis [25].

3. Different bio-inspired fouling resistance surfaces

3.1. Lotus leaves effect

3.1.1. Natural structure. Lotus symbolized holiness and purity in ancient Chinese and Indian cultures, which means that human beings have long discovered the resistance of this plant to fouling. From the perspective of physiological needs, the self-cleaning property is necessary for the lotus to maximize the efficiency of photosynthesis since the environment in which the lotus thrives is usually swampy and wet, which leads to a higher probability of dust attachment and bio-fouling.

The mechanism behind the properties of lotus leaves surfaces for water-resistance, and self-cleaning is the high contact angle with water droplets (>150°), i.e., superhydrophobic. Besides, the lotus leaves have low hysteresis, which leads to a low sliding grade (<2°), allowing for droplets to slide down easily [26]. As Fig.7 shows, these sliding droplets collect any debris on the leaf's surface, thus providing a natural self-cleaning property. This is known as the "Lotus Effect" [27].

With the help of a scanning electron microscope (SEM), the unique structure of lotus leaves can be revealed, as shown in Fig.8. Two hierarchies assemble the whole system. Fig.8.(c) shows the hills (papillae) and valleys on the micron scale, which is the second hierarchy. Due to the large water droplets, the valley areas are inaccessible to them. The attached nanoscale wax tubes on hills and valleys in Fig.8.(d) are regarded as the first hierarchy, which has a repelling nature. As mentioned before, the debris will be pushed up and then collected by water droplets [27]. In addition, it is analyzed that the adhesion between water and surfaces can be reduced significantly by structural hierarchy while providing a larger apparent contact angle, reducing the contact area and the length of the contact line [28]. That also explains why lotus has such a large contact angle and the transcendental superhydrophobic characteristic (Figures 7 and 8).

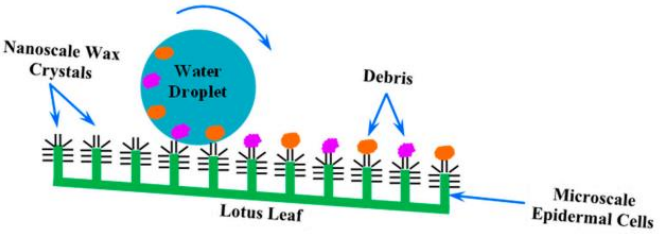

Figure 7. Simple schematic of the lotus effect [27].

DOI: 10.54254/2755-2721/7/20230409

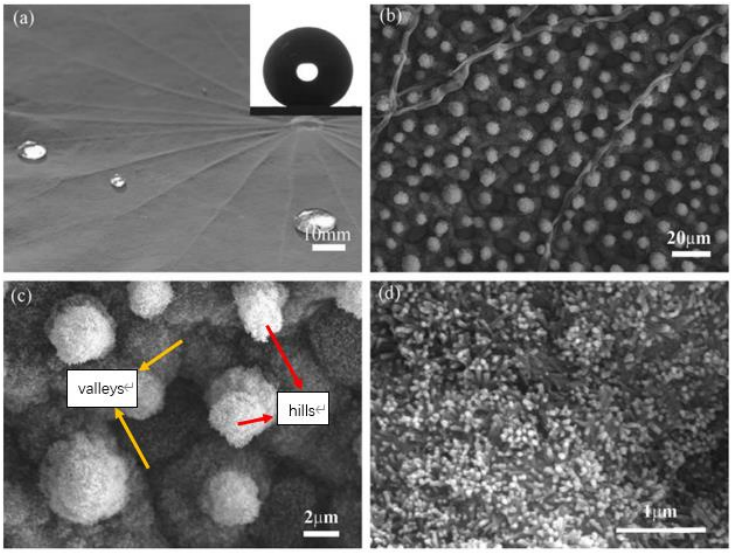

Figure 8. The surface structures of lotus leaf at different scales (modified from [29]) (a) droplets on the surface. (b) and (c): the microscale surface structure of lotus leaf. (d) the wax tubes on the leaf.

3.1.2. Applications for anti-biofouling. Inspired by the unique structure of the lotus leaf, many superhydrophobic micro-nano hierarchical scale surfaces materials are developed and applied in fouling resistance [30]. One of the most promising application areas is anti-biofouling. It is widely believed that diseases related to medical devices caused by bacterial infections have become a severe growing threat to global healthcare [31]. Some sterilization methods, like using antibiotics, could be influenced by the resistance evolution of bacteria under natural selection, which will cause a rapid loss of effectiveness and trigger antimicrobial resistance [31]. Therefore, developing a new material with anti-biofouling is recognized as a constructive approach. Among all the natural bio-inspired surfaces, the nanostructure of lotus leaves shows impressive anti-bio-fouling properties. Jiang et al. used Gram-negative E. coli as the representative microorganism and observed that the bacteria adhered to the surface of lotus leaves are highly deformed to death. It is proved that the demise of bacteria can be attributed to the stretching of the cell membrane caused by the wax nanotubes on the surface of a lotus leaf. Inspired by this phenomenon, a series of hierarchical surface materials with silicon micron scale cylinders and ZnO nanoneedles are developed (shown in Fig.9. and Fig.10.). These materials are then treated with fluoroalkyl silane to render low surface energy and deliver an anti-bacterial performance than the non-treated surface. [31] (Figure 9 and Figure 10).

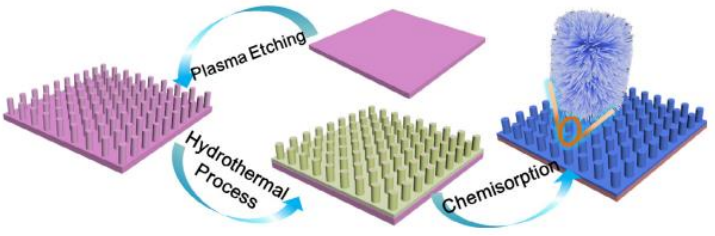

Figure 9. Schematic illustration of developing imitation lotus leaf surface structure material [32].

DOI: 10.54254/2755-2721/7/20230409

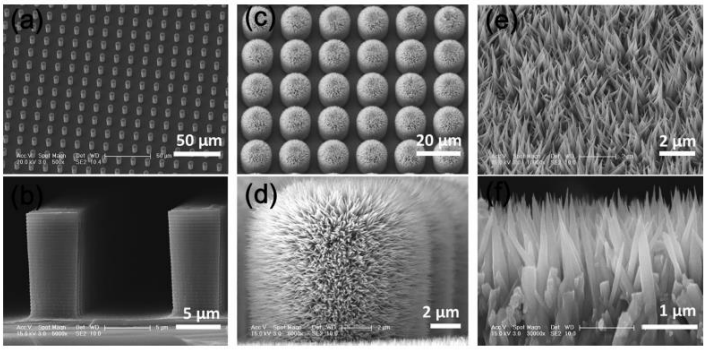

Figure 10. SEM images of lotus leaf-liked materials. (a) and (b): microscale structure patterned silicon surface (MS). (c) and (d): dual-scale structures patterned cover (DS). (e) and (f): pure nanoscale structure patterned cover (NS). [31].

In bactericidal experiments, the dual-scale structures which imitated the lotus leaf showed the best anti-bacterial characteristics (Fig.11.). After 24 h incubation, more than 99% of bacteria were eliminated on the surface compared to the silicon wafer [31]. This indicates that lotus leaf-inspired materials have excellent potential in applicating in anti-bacterial areas such as medical devices (Figure 11).

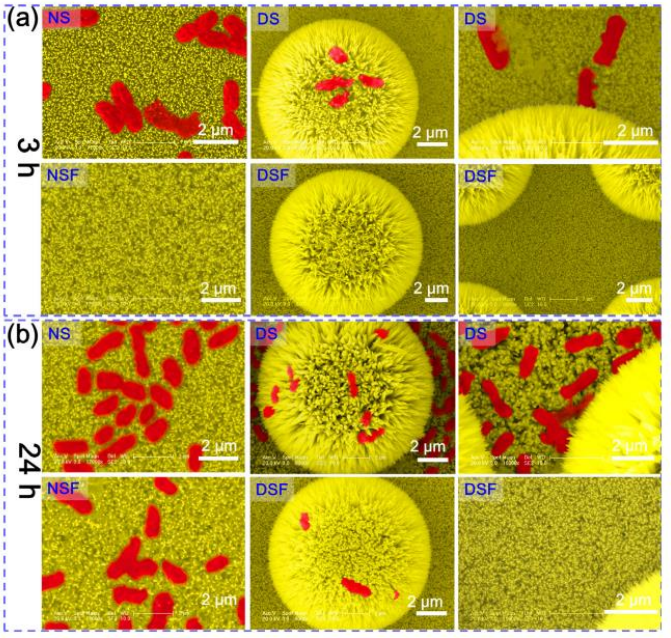

Figure 11. SEM images about the morphologies of E. coli cells adhered on different material samples after three h (a) and 24 h (b) incubation [31].

3.1.3. Applications for other fouling resistance. In addition to biofouling, lotus-inspired surfaces have also produced a marked effect on other types of fouling resistance. One of the examples is ice-fouling. The unwanted ice accumulation on surfaces affects commercial and residential activities, causing an expensive problem for many major industries [32]. Among the problems caused by icing, many are due to the striking of supercooled water droplets onto a solid surface. Ice formed in this way is infamous for breaking tree limbs and power lines, glazing roadways, and stalling aircraft airfoils, which may cause tremendous economic losses [33]. According to Rajiv et al. [34], synthetically fabricated surfaces composed of multi-walled carbon nanotubes (MWCNTs) and carbon nanofibers (CNFs) can be used as a coating to reduce ice fouling significantly. After further processing using

DOI: 10.54254/2755-2721/7/20230409

supercritical fluid (SCF) to protect the material from damage at low temperatures, the new composite (SCF–MWCNT–CNF) showed excellent superhydrophobicity and anti-icing performance. Using a group of uncoated fiber-reinforced polymer sheets (FRP) and a group of FRP sheets with the composite coating (SCF–MWCNT–CNF) as the control experiment, controlling other variables and placing them under supercooled water, it can be observed that there is almost no icing on the coated FRP plate (Fig.12.). Therefore, the coating could be a possible and efficient way to prevent ice fouling caused by striking of supercooled water droplets (Figure 12).

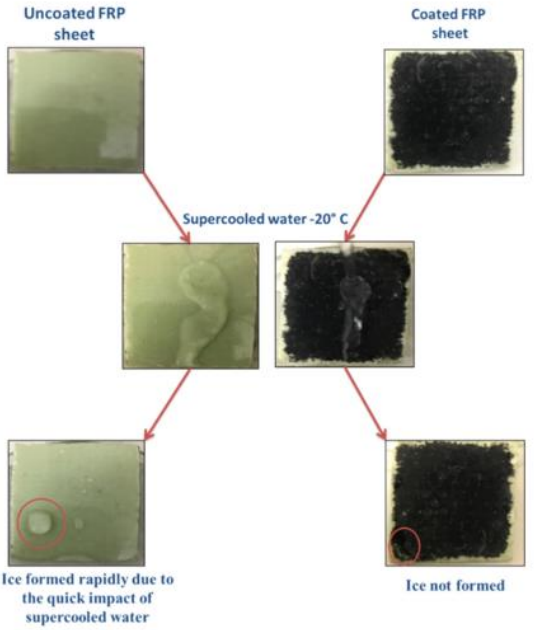

Figure 12. The anti-icing test images of the uncoated and coated FRP sheets [34].

The SCF–MWCNT–CNF also showed healthy resistance against dirt (Fig.13.). The adhered dirt can be washed away by water droplets sliding on the coating surfaces and leaving a well-cleaned surface [34] (Figure 13).

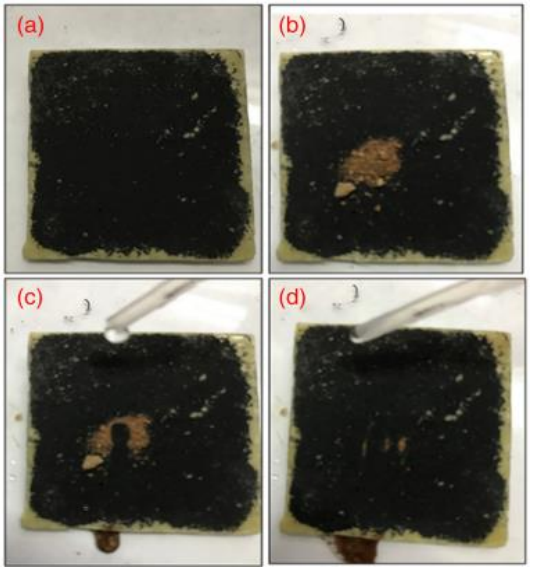

Figure 13. Fouling resistance experiments for the SCF–MWCNT–CNF surface: (a) clean surface, (b) surface with dirt, (c) adding water droplets on the defiled surface, (d) the surface after the water-pouring procedure. [34].

DOI: 10.54254/2755-2721/7/20230409

Materials inspired by the lotus effect can also be used for precipitation fouling resistance. With the progress of industrialization and population growth, the water shortage has become a more severe problem, and seawater desalination technology is regarded as one of the solutions [24]. One of the promising desalination technologies is membrane distillation (MD) which is widely used for recovering the water and concentrating the brine after using reverse osmosis to treat a feed solution [24]. However, the accumulation of salt fouling, like sodium dodecyl sulfate, significantly reduces the membrane's robustness [35].

A modified polyvinylidene fluoride (PVDF) superhydrophobic membrane inspired by the lotus effect for robust membrane distillation was developed by Hou *et al.* [35]. The spherical polyvinylsilsesquioxane (PVSQ) nanoparticles are grafted onto micron-sized silica particles (SiPs) to obtain the hierarchical micro-nanoscale texture on the membrane surface, which plays a vital role in fouling resistance (Fig.14. and Fig.15.). The hydrophobic groups including methoxyl and vinyl formed from the condensation reaction of the vinyltrimethoxysilane (VTMOS) helps to diminish the membrane surface energy (Figure 14 and Figure 15).

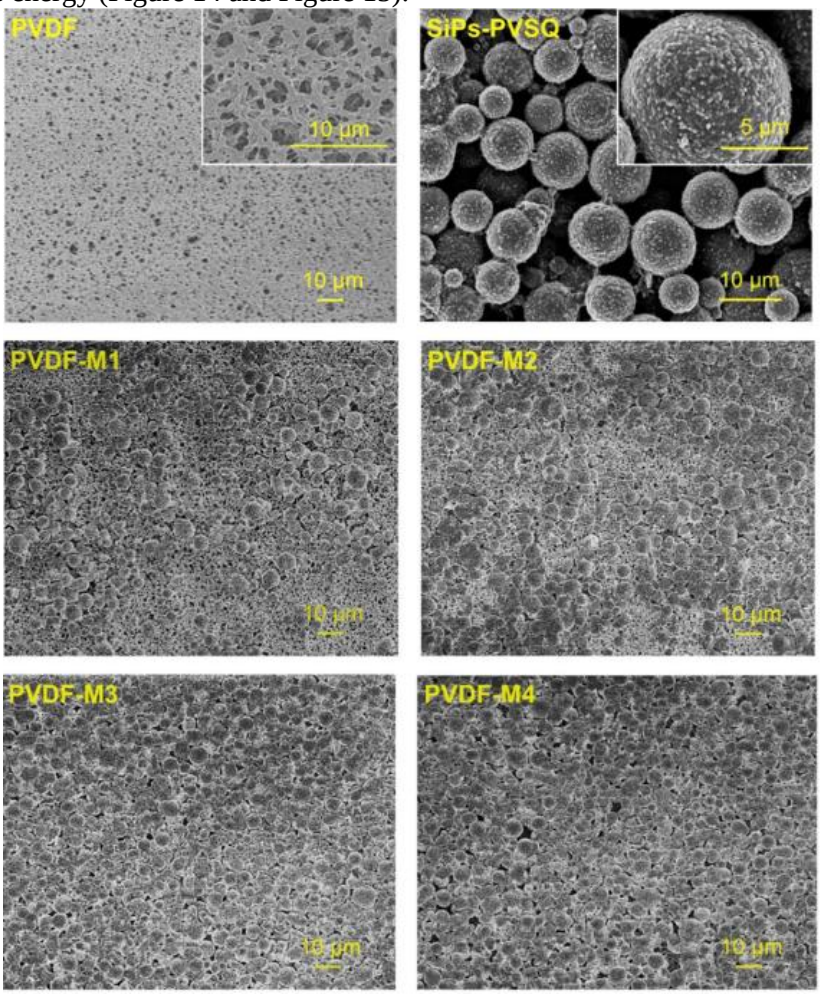

Figure 14. SEM images of the SiPs-PVSQ composite particles and the commercial PVDF membrane surfaces with modified membranes. [35].

DOI: 10.54254/2755-2721/7/20230409

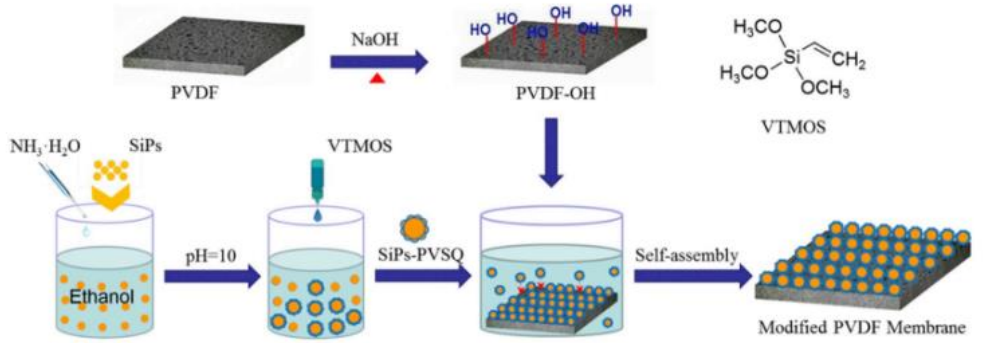

Figure 15. Schematic demonstrating the process of surface modification of a commercial membrane [36].

Using a solution including NaCl (100 g/L), CaCl2 (20 mM), and HA (50 mg/L) as reagents and comparing the anti-fouling performance of pristine PVDF with modified PVDF-M3, it is observed clumpy deposits highly covered the former one. In contrast, the PVDF-M3 membrane is almost free of such fouling (Fig.16.), which indicated the robust fouling resistance of modified PVDF [35] (Figure 16).

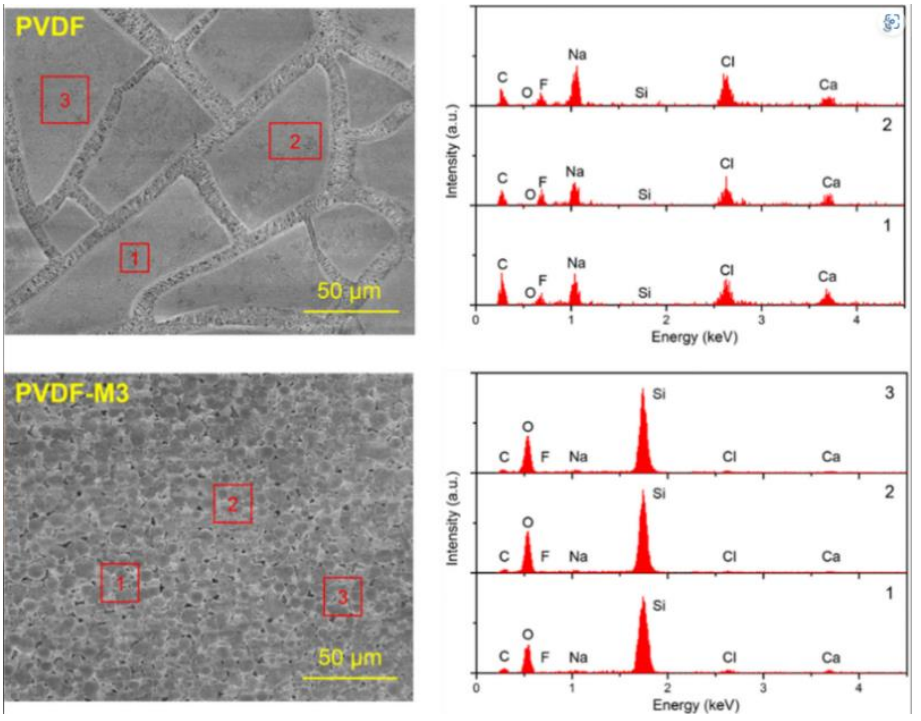

Figure 16. SEM-EDS analysis of the two different membrane surfaces after the experiments mentioned above [35].

3.2. Shark skin effect

3.2.1. Structure. Shark skin is another famous surface with transcendental fouling resistance. During swimming at high speeds, the shark skin plays a vital role in reducing the fluid drag, which helps it to catch prey. It can also protect it from the adhesion of biofouling, such as barnacles or some microorganisms. The unique surface microstructure on shark skin surfaces explains this phenomenon [19].

DOI: 10.54254/2755-2721/7/20230409

Shark skin is composed of tiny rectangular scales (Fig.17). The scales are shield scales called dermal denticles, which are tooth-like and arranged in an orderly and compact way. The tips of these fine scales are uniformly oriented. Besides, its scales are attached to spines and bristles, called the riblets structure [37]. These sophisticated structures optimize the control of the turbulent vortex, diminishing shear stress and momentum transfer, which further leads to drag reduction. The low drag also promotes the fluid flow at the skin, making it harder for an organism to colonize and contributing to its biofouling resistance [8] (Figure 17).

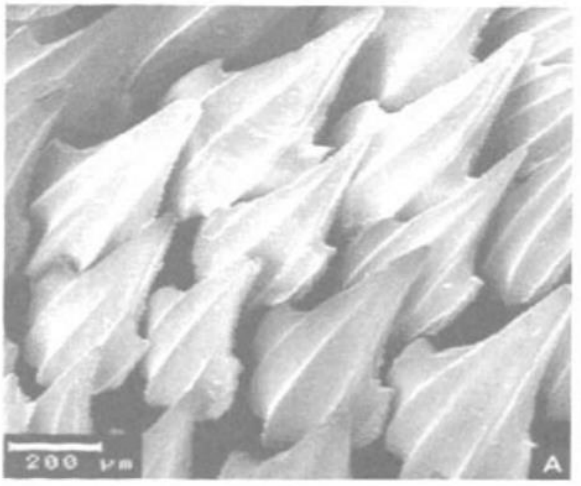

Figure 17. The scale of shark skin [38].

3.2.2. Application of ship protection. On a ship's hull, there are often some humus and mud on it, which could attract some algae and shellfish. A shark skin-inspired ship coating called Gator Sharkote can significantly diminish the sedimentation and colonization of various seabed biological spores, such as algae and Ulva, which are expected at the bottom and sides of the ship, by 85% (Figure 18).

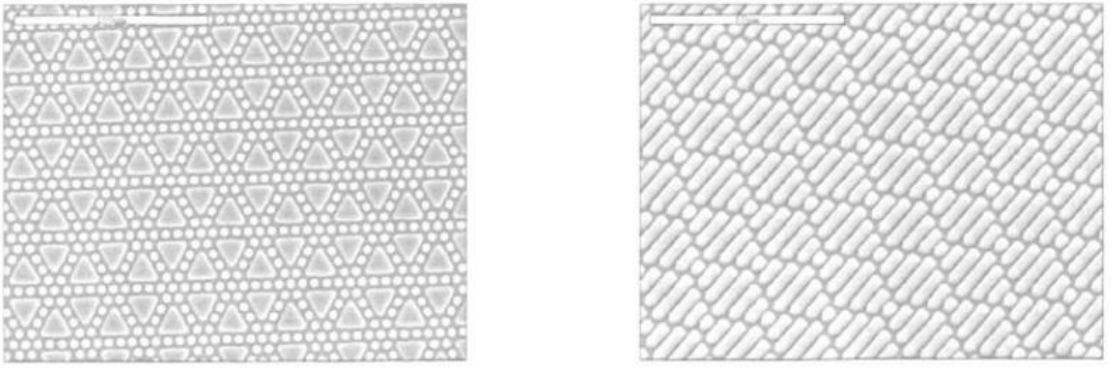

Figure 18. A type of ship coating innovation based on shark skin [37].

Gator Sharkote uses plastic and rubber material to copy shark skin and is made with billions of diamond-shaped protrusions. There will be some other protrusions on the diamond-shaped protrusions.

The working mechanism for this kind of coating needs a small power current. When the small power current acts on the surface, the pattern of diamond-shaped protrusions will start to change and bulge or retract. When this happens, the hull's character will also begin to bulge or abandon and throw the humus and mud away. As a result, there will be less humus and dirt on the surface, adhesion amount of seaweed, rattan gourd, and shellfish will also decrease.

DOI: 10.54254/2755-2721/7/20230409

3.3. Pilot whale skin

3.3.1. Biomimetic whale skin for the antifouling application. The pilot whale's (Globicephala melas) skin is devoid of tiny biofuels and has a spotless appearance. [40] The surface of Globicephala melas is encircled with nano-ridge holes, which are significantly smaller than other marine biofuels (diameter 0.2 m), as seen in Fig. 1.b. Baum et al. concluded that microorganisms could connect to the skin only at the edges of pores or the peak of nanoridges.

It is clear from earlier research that the uneven distribution of epidermal desquamation and cellular architecture is to blame for the smoothness of surfaces [39,40]. Zymogel, present in pilot whale skin, hydrolyzes microorganisms to prevent buildup [40]. The stratum corneum's hydrolytic enzyme gels stop biofuels from adhering. Zymogel is a hydrophilic bio gel created by aggregate-attached enzymes from the desmosomal junction system. [17]

It's noteworthy to note that the skin of the pilot whale can act as an amphiphilic surface since it includes both polar and non-polar groups. [41] X-ray photoelectron spectroscopy (XPS) measurements show the existence of both polar and non-polar groups. (fig.20) On the same surface, it results in opposing wettability. The coating on the surface, which is made up of lipids (hydrophobic) and gel-like materials filling the pores (hydrophilic), caused a significant decrease in both short-term and long-term fouling, as seen in (fig.20.a) under cryo-scanning electron microscopy (CSM). [42]

Furthermore, the presence of hydrolytic enzymes supports the self-cleaning mechanism of the whale skin surfaces;. However, it is unknown that the relationship between the efficiency of rate-dependent desquamation and the efficiency of rate-dependent adhesive biofuels; there is an assumption that the desquamation process depends on hydrolytic enzymes within the intercellular region, as the hydrolytic enzymes can hydrolyze the contaminants.[42]

Hydrolytic enzymes further support the self-cleaning mechanism of whale skin surfaces. Although the relationship between the effectiveness of rate-dependent desquamation and the effectiveness of rate-dependent adhesive biofuels is unknown, it is assumed that the desquamation process depends on the presence of hydrolytic enzymes in the intercellular region because these enzymes can hydrolyze the contaminants. [42]

During the high-speed movement, the gels display the characteristics of a viscoelastic solid, which can withstand the high shear during jumping and promote the desquamation of epidermal cells to self-polish. [40] The flow of water increases the fluidity of the biofuels (Fig.19.a), Baum et al. suggested a new model on the skin surface, adhesive polymers can be disassembled by the high-speed water flow, that the retention of fouling on the surface can be reduced when the detaching force increased. [42,43]. The air bubbles contacting with smooth surfaces can broaden the ability to remove the particles.[42]

Pilot whales, as previously mentioned, desquamate their epithelial cells to enable self-polishing; this mechanism stimulated the development of self-polishing copolymers. Additionally, pilot whales' skin exhibits a self-cleaning property because they remove minor fouling through enzymatic digestion. The undersea circulatory system may be used in situ to produce protective coatings. These liquid components can combine to create a dense layer that can adjust to seawater's pH and salinity changes. The skin will then disintegrate in the waves, clearing the pollution. [30] (Figure 19 and Figure 20, and Figure 21).

DOI: 10.54254/2755-2721/7/20230409

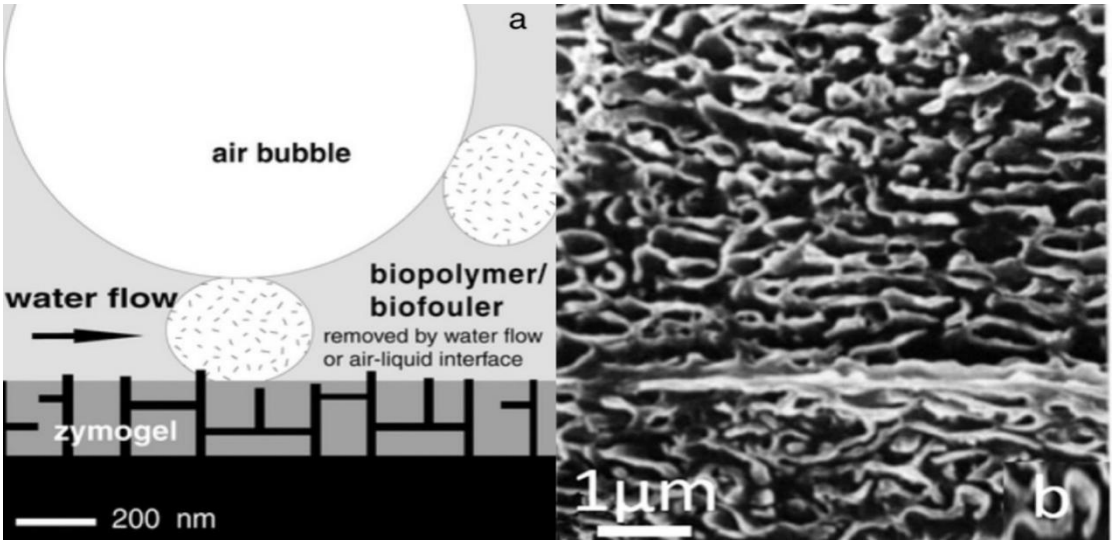

Figure 19. (a) the model of the self-cleaning abilities of pilot whale skin.[2-4] (b) the SEM micrograph nano ridges and pore's structure [40].

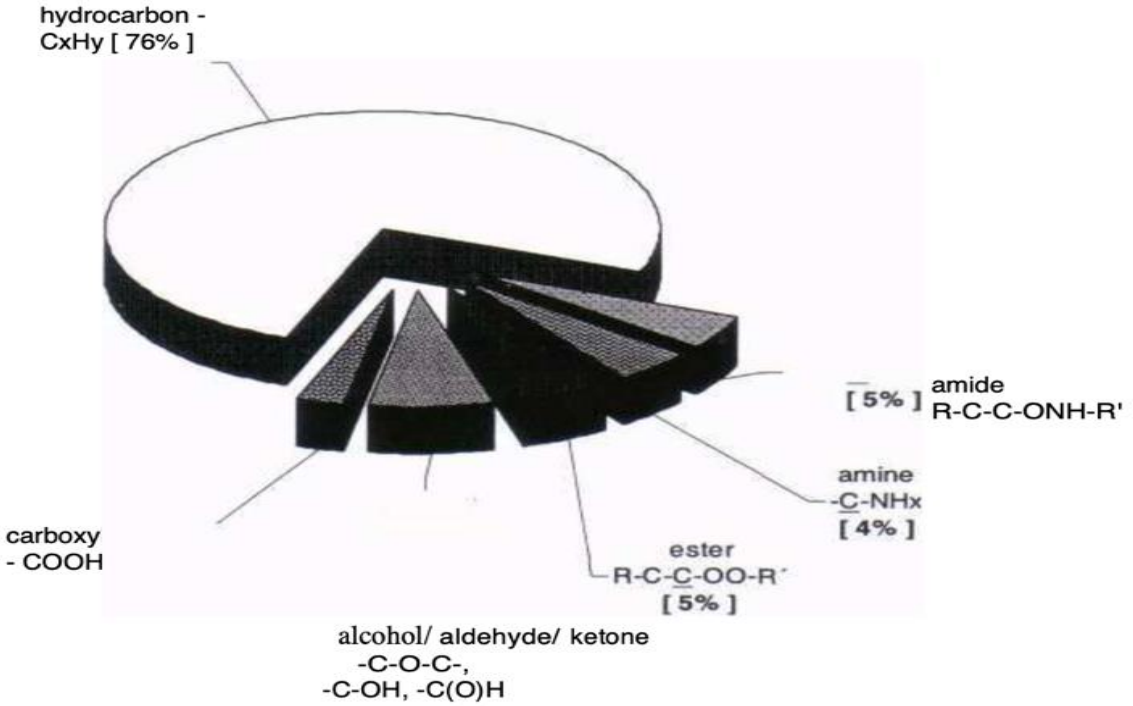

Figure 20. The distribution of polar and non-polar groups on globicephala melas [42].

DOI: 10.54254/2755-2721/7/20230409

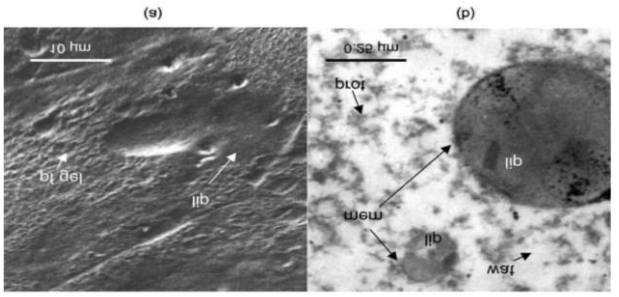

Figure 21. (a) CSM micrograph of the skin surface of G Globicephala melas, pf gel means pore-filling gel, and the lip means lipid. (b) TEM micrograph of proteinaceous gel components and membrane-coated lipid droplets. [42]

3.3.2. Self-polishing copolymers. These fouling-free surface coatings comprise polymers that may hydrolyze and dissolve in saltwater and are based on acrylic or methacrylic copolymers. [44] Due to tributyltin's (TBT) biotoxicity and subsequent use prohibition, new self-polishing copolymers (SPCs), such as zinc methacrylate (ZMA), copper methacrylate (CMA), and triisopropylsilyl acrylate, were created (TIPSA). [45] However, ZMA and CMA displayed higher adsorption energy and lower activation energy than TIPSA, suggesting that they may be polished more quickly than TIPSA. Understanding how ZMA, CMA, and TIPSA molecules degrade in saltwater is essential for finding the best antifouling materials. [45]

Figure.6 shows that the whole decomposition mechanism of SPCs is divided into three different sections. Each pendant group will decompose after contact with seawater's Na^+ and Cl^- ions. Furthermore, they also can be spoiled by the OH^- ions in seawater.[45] In the initial stage, the presence of Na^+,Cl^- andOH^- indicates that these ions are adsorbed by SPCs molecules, and Na^+tends to be close to the oxygen sites, while the other anions tend to be close to the pendant groups. In the next stage, NaCl and NaOH dissociate and bind to the site between oxygen and pendant atoms to decompose functional groups; then, the dissociated ions remain at the decomposition sites. At the final stage, there is a strong connection among the anions, the oxygen atoms, the pendant groups, and the Na^+ions. [45] (Figure 22 and Figure 23).

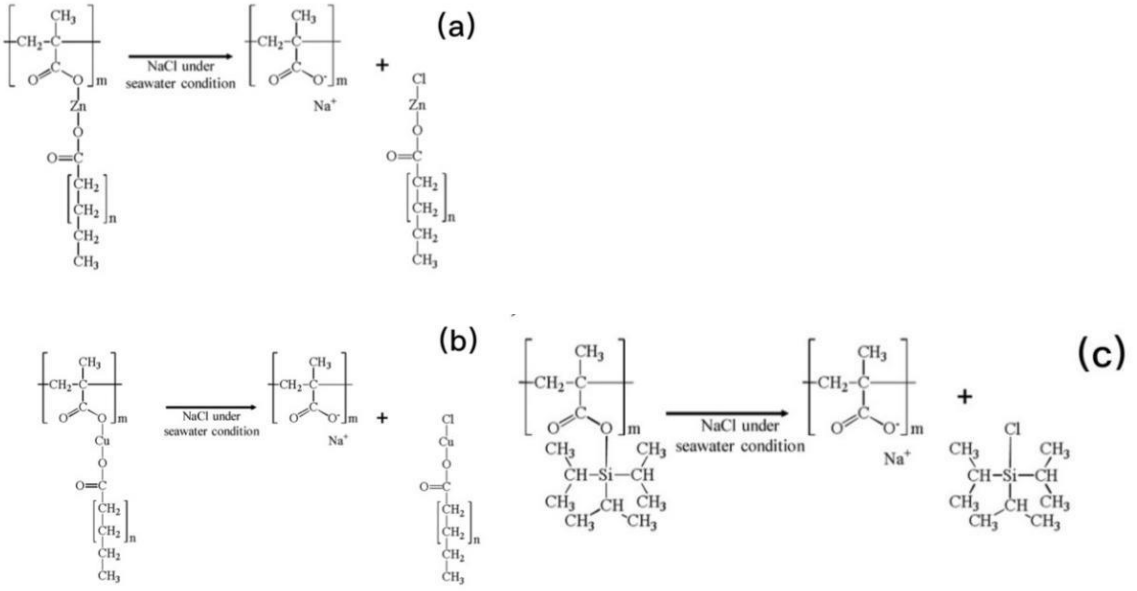

Figure 22. The decomposition mechanism of distinct SPCs under seawater: (a) ZMA (b) CMA (c) TIPSA [45].

DOI: 10.54254/2755-2721/7/20230409

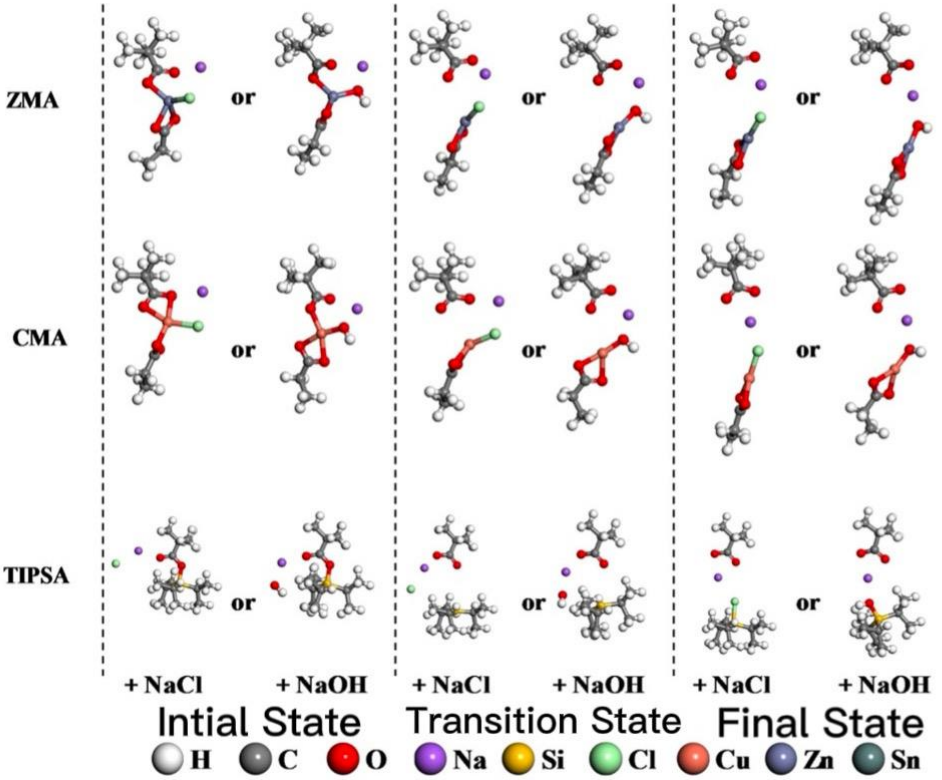

Figure 23. Different stages of the decomposition mechanism of ZMA, CMA, and TIPSA polymers.[45]

Moreover, the different adsorption energies help identify the energy variation during decomposition. The adsorption energy of ZMA, CMA, and TIPSA is -3.13eV, -2.68eV and -1.44eV in NaOH, respectively. And the adsorption energy of is -1.77eV, -1.28eV and -0.92eV in NaCl, respectively. OH^- ions have a more vital absorption ability for pendant groups than Cl^-. Regarding activation energy, different functional groups and atomic species in the pendant group show different activation energies. The activation energies of ZMA are 1.36eV in NaCl and 1.14 eV in NaOH, while CMA offers a lower value, 0.94eV in NaCl and 0.72eV in NaOH. The highest one is TIPSA, 2.70eV in NaCl and 2.65eV in NaOH. The activation energy of SPC molecules with NaOH is lower than that of SPC molecules with NaCl. Additionally, since ZMA and CMA SPC molecules showed lower activation energy, these molecules can be polished faster than TIPSA SPC molecules. So these two molecules are appropriate for antifouling agents. [45](Figure 24)

DOI: 10.54254/2755-2721/7/20230409

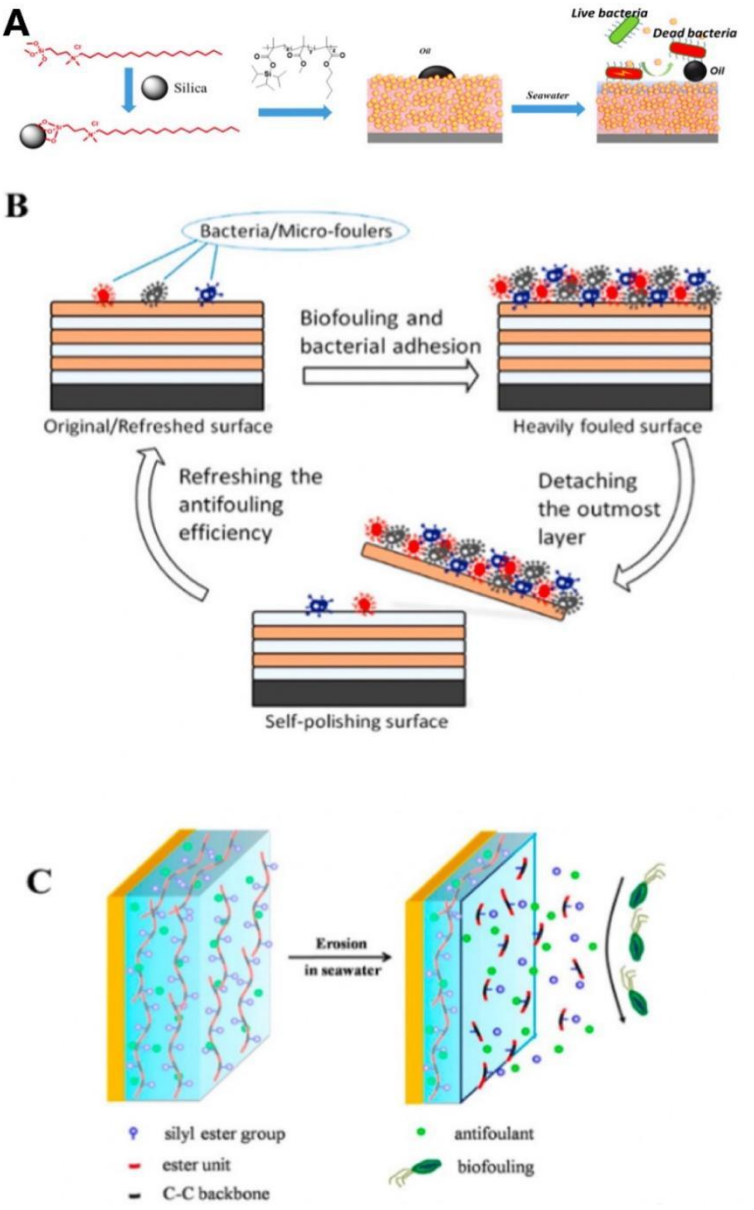

Figure 24. (a) dimethyloctadecy [3-(trimethoxysilyl) propyl] ammonium chloride was bound with SiO_2 to produce $QAS-SiO_2$, then combined with a self-polishing polymer.[39] (b) combining dextran aldehyde (Dex-CHO) and carboxymethyl chitosan (CMCS) through layer-by-layer deposition in aldehyde-amine reactions.[46]

(c)The antifouling surfaces with MDO. [47]

SPCs without biocide release that is more ecologically benign have recently been researched and produced. [43] According to D. Wang et al., a self-polishing polymer should be combined with dimethyloctadecyl [3-(trimethoxysilyl) propyl] ammonium chloride, which is bound with SiO2 to generate QAS-SiO2. (Fig.24.a) As SiO2 nanoparticles are inexpensive and may hydrolyze and dissolve in basic environments, SPCs are suitable building blocks for creating micro/nanostructure surfaces in coatings. Additionally, this micro/nanostructure has bactericidal and self-renewing properties. [39]

To accomplish antifouling and antibacterial adhesion, Xu et al. mixed two polysaccharides, dextran aldehyde (Dex-CHO) and carboxymethyl chitosan (CMCS), by layer-by-layer deposition in aldehyde-

DOI: 10.54254/2755-2721/7/20230409

amine processes. These two properties have improved when there are more Des-CHO/CMCS bilayers due to the hydrophilicity's expansion and the decrease in surface roughness (Fig.24.b). [20] In an acidic environment, the capacity for self-polishing has also increased. Bactria production increases when the environment becomes more acidic, which increases the rate of self-polishing.[44]

To accelerate the erosion of traditional SPC [44], Zhou et al. developed anti-biofouling materials by combing 2-methylene-1,3-dioxepane (MDO), tributyl silyl methacrylate(TBSM) and MMA. The polymer's backbone is degradable and hydrophobic, which improves its ability to self-polishing and decreases its swelling. Without shear force, the polymer can degrade quickly, so its antifouling ability increases in static conditions. (Fig.24.c) The copolymer with MDO can inhibit biofouling, and the mechanical properties have been improved in the marine environment.[47]

3.4. SLIPS

3.4.1. Structure inspired by the pitcher plant. Since pitcher plants usually survive in nutrient-poor environments, they generate specialized leaves to trap and digest prey to support growth [48]. The key point for successful hunting is its peristome. The game can touch the peristome and eat the nectar while it is dry. However, as the pitcher plant becomes active, water condenses on the peristome to form a homogeneous thin film so slippery that the prey falls into the digestive zone [49]. A light water film can develop because of the peristome's hierarchical structure, as shown in Fig.25. These hierarchical structures increase the roughness of the surface. As shown in the Wenzel model and the Cassie-Baxter model, roughness increases, the hydrophilic surface becomes more hydrophilic, and the hydrophobic surface becomes more hydrophobic. As shown in Fig.26, the hydrophilic nectar and the hierarchical structure provide a super-hydrophilic characteristic for the peristome surface (Figure 25 and Figure 26).

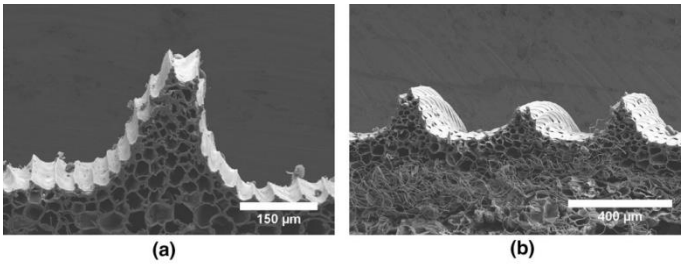

Figure 25. Hierarchical structure of the peristome surface. (a) individual, and (b) a series of ridges on the surface. Image adapted from reference [49].

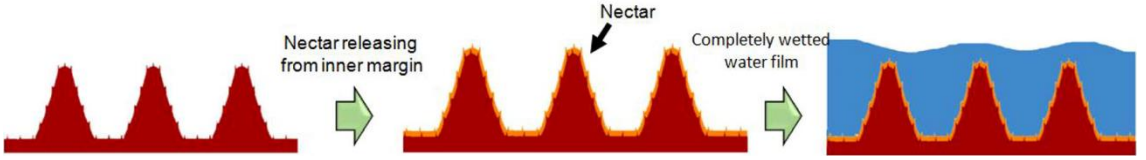

Figure 26. Water film formation on the peristome surface. Image adapted from reference [49].

Slippery liquid-infused porous surfaces (SLIPS), which are established as depicted in Fig. 27, are modeled after knowing the structure of the pitcher plant: Low surface tension liquid, often known as a lubricant, and functionalized porous solid are combined. The SLIPS should have unique characteristics: (1) low contact angle hysteresis, (2) low sliding angle, (3) repeatable self-healing, and (4) high-pressure stability. [50] (Figure 27)

DOI: 10.54254/2755-2721/7/20230409

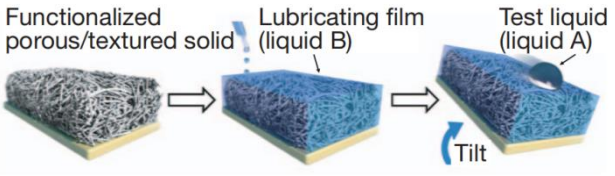

Figure 27. Schematics indicating the fabrication of a SLIPS. Image adapted from reference [50].

3.4.2. Application on anti-icing. Icing can sometimes lead to catastrophic problems. For example, ice that accumulates on the aircraft may cause it to crash [51]. Discovering a new way to remove or avoid ice is essential to research. Some techniques can remove ice fouling but are too expensive to be widely utilized. Compared to the deicing process, directly preventing ice formation is more effective. Due to the short experimental contact time between the water droplet and the cold substrate, superhydrophobic surfaces modeled after knowing the structure of the lotus leaf have recently been observed to have good anti-icing properties [29]. However, the superhydrophobic coating is not always icephobic. Under high humidity, the anti-icing efficiency is low, and the water condenses on a superhydrophobic surface and then gets interlocked with the porous structure of the surface once it freezes [52]. In this case, SLIPS have attracted a lot of attention as an alternative to superhydrophobic surfaces since it has very low contact angle hysteresis and the water that condenses on it can be quickly removed by slightly leaning the surface, as shown in Figure 28 and Figure 29.

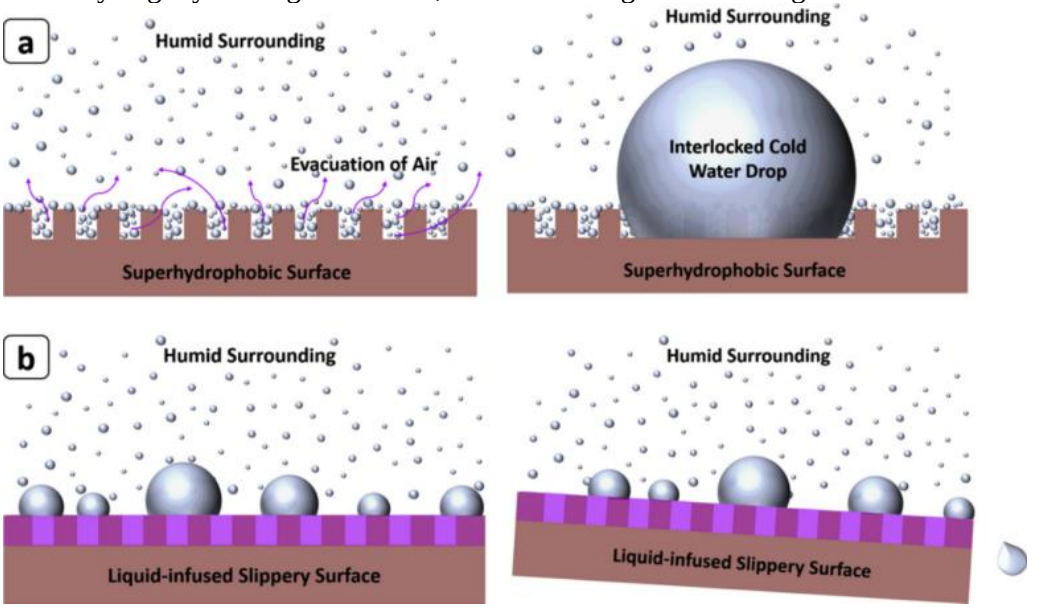

Figure 28. Schematic showing anti-icing efficiency under high humidity of (a) superhydrophobic surface and (b) SLIPS. Image adapted from reference [51].

DOI: 10.54254/2755-2721/7/20230409

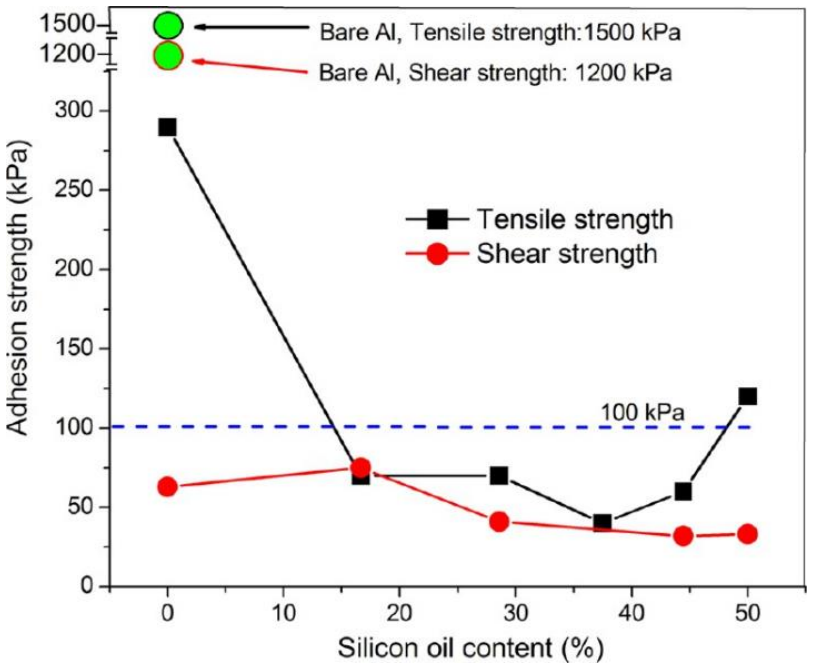

Figure 29. Ice adhesion’ s tensile and shear strength on the PDMS coating surfaces with various percentages of silicon oil content. Image adapted from reference [53].

Irajizad et al. [32] described the functional icephobic surfaces should have the following four properties: (1) low ice formation temperature, (2) slow ice accumulation rate, (3) low ice adhesion strength at the ice-solid interface, and (4) high durability. Zhu et al. [53] discover that with the specific content of the silicon oil as a lubricant, the ice adhesion of silicon-oil-infused polydimethylsiloxane (PDMS) coatings changes, as shown in Fig.29. When the ice adhesion is lower than 20 kPa, natural forces like the wind can remove the ice from a surface. In this case, PDMS coating surfaces can be icephobic solid materials. Zhang et al. [54] produce a double-layered SLIPS coating on Mg alloy, as shown in Fig.30, consisting of the water-repellent lubricant, a top layer made of the self-assembled monolayers (SAMs), and an underlayer made of the LDH−carbonate composite. This double-layered SLIPS exhibits anti-icing ability and long-term icephobicity, as shown in Fig.31, which is essential for practical applications (Figure 30 and Figure 31).

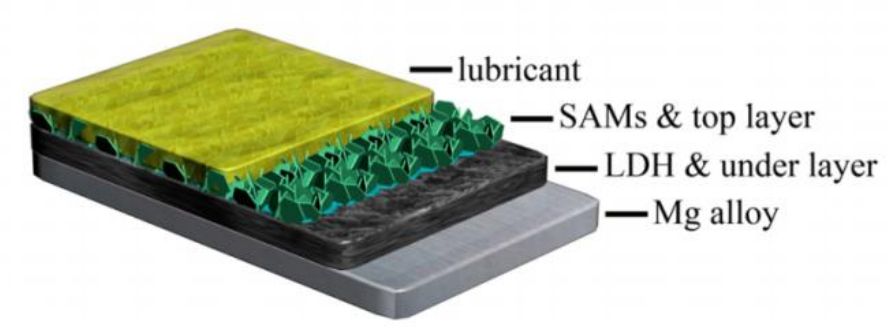

Figure 30. Schematic of the double-layered SLIPS. Image adapted from reference [54].

DOI: 10.54254/2755-2721/7/20230409

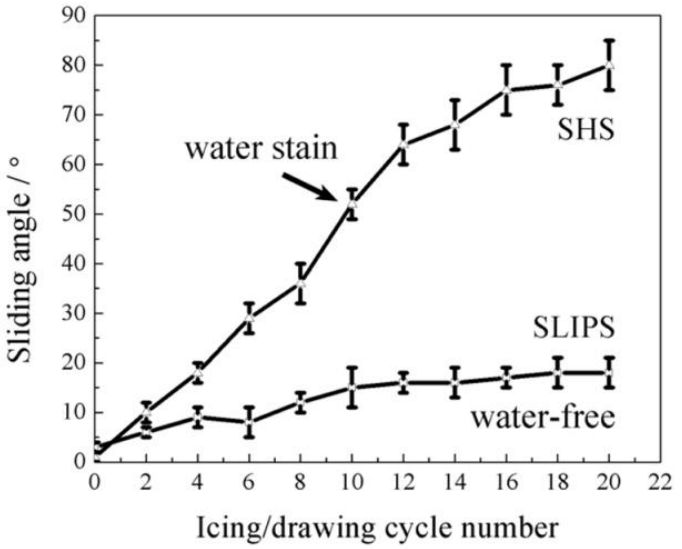

Figure 31. Variations in the SHS and SLIPS sliding angles during the test cycles. Image adapted from reference [54].

3.4.3. Application of other fouling. In addition to anti-icing, SLIPS also has an anti-biofouling performance. Biofouling produces a lot of trouble for the marine industry. For a typical marine biofouling organism, Chlorella Vulgaris, Wang et al. [55] prepare special SLIPS to resist it through anodization of aluminum, modification with FOTS (1H,1H,2H,2Hperfluorodecyl trichlorosilane), and lubricant infusion with PFPE (Perfluoropolyether). As shown in Fig.32, C. Vulgaris accumulates on the bare aluminum (Fig.32a). On the contrary, fewer C. vulgaris settles onto the SLIPS during the experiment (Fig.32b). Compared to organic biocides and toxic anti-biofouling coatings with metal, SLIPS is more environmentally friendly and has potential for anti-biofouling application [55] (Figure 32 and Figure 33).

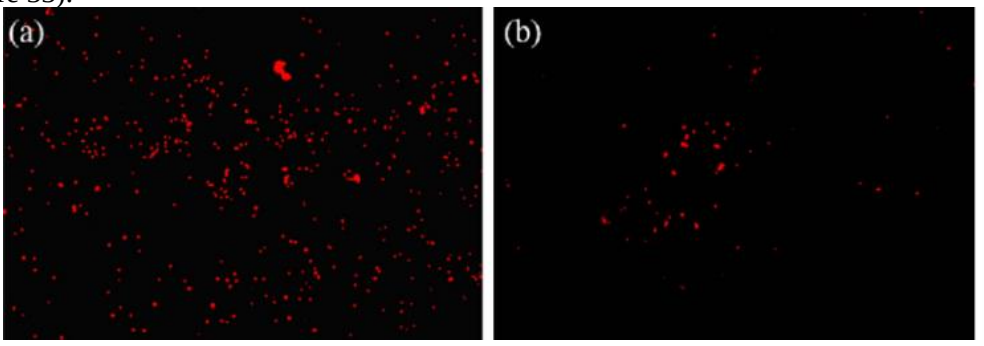

Figure 32. Fluorescent micrograph chlorella vulgaris settled on (a) bare aluminum and (b) SLIPS. Image from reference [55].

Mold fouling in the tire industry is another one in which SLIPS shows an anti-fouling performance. Rubber can stick to the mold surface and deposit a coating that blocks heat transition during the vulcanization process, leading to additional energy costs and damaged equipment [56]. Liu *et al.* [56] designed SLIPS on aluminum alloy by anodic oxidation, myristic acid modification, and infusion with Krytox GPL104 perfluorinated oil. The difference among mold fouling resistance of native aluminum alloy (NAT), anodized surface (AS), superhydrophobic surface (SH), and SLIPS is shown in Fig.33. At the same time, a self-cleaning property and stability under high pressure and temperature reveal that SLIPS is a potential strategy to resist mold fouling.

DOI: 10.54254/2755-2721/7/20230409

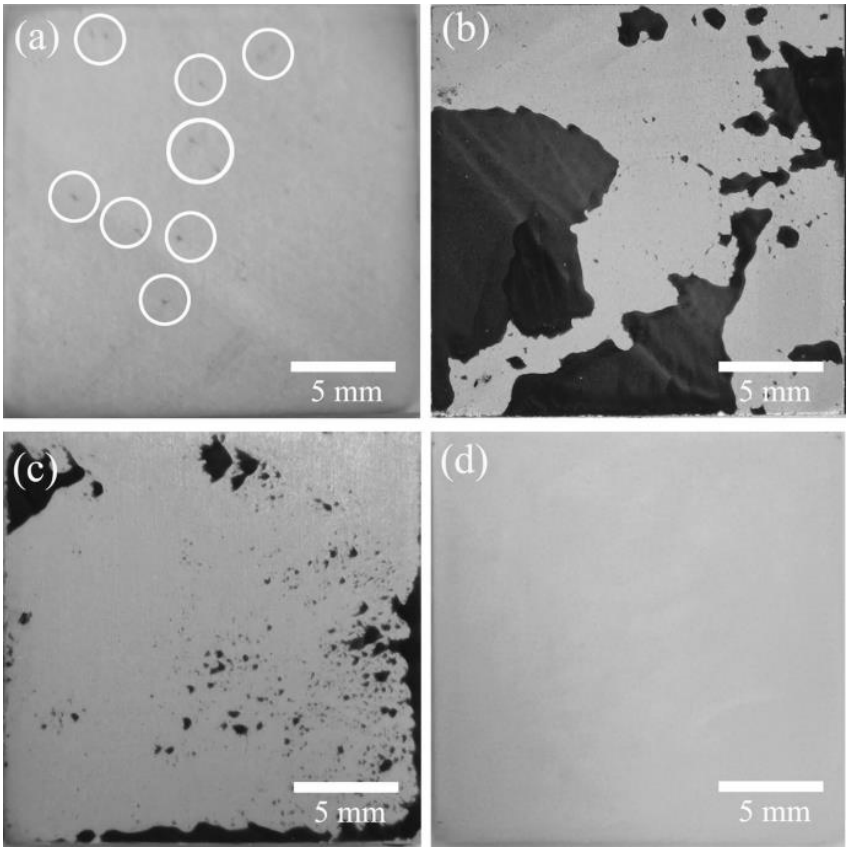

Figure 33. Black and white contrast graphs of the vulcanization test results for (a) NAT, (b) AS, (c) SH, and (d) SLIPS. Image adapted from reference [56].

3.4.4. Improvement for SLIPS

Tenjimbayashi *et al.* and Wang *et al.* [57,58] indicate that SLIPS still has the following limitations: (1) lubrication is likely removed through contact or evaporation, which is unfavorable for a long-term application; (2) the fabrication process has to be shortened, not only for lower cost but also for applications like a pressing surgery operation; (3) it is hard to coat specific substrates and small surfaces.

For the first part, Zhang *et al.* [59] point out that infusing lubricant into tube-like SiO_2 composite structure produces robust slippery surfaces with a low evaporation rate, 0.08%/day with Krytox104 lubricant. As shown in Fig.34, lubricant oil can be locked in identical porous tubes. Additionally, the microporous structure of the tube wall shown in Fig.34e results in a self-replenishing property. When the lubricant on the upper surface was removed, those in a microporous structure permeated outward to repel the liquid.

For the rest part, instead of multiple, time-consuming steps, a lubricated fiber-filled porous sheet is provided by Tenjimbayashi *et al.* [57], and attaching a surface to the sheet can easily get a coating as shown in Fig.35. Since this technique focuses on small areas coating, it aids in the creation of functional surfaces such as endoscope lenses (Figure 34 and Figure 35).

DOI: 10.54254/2755-2721/7/20230409

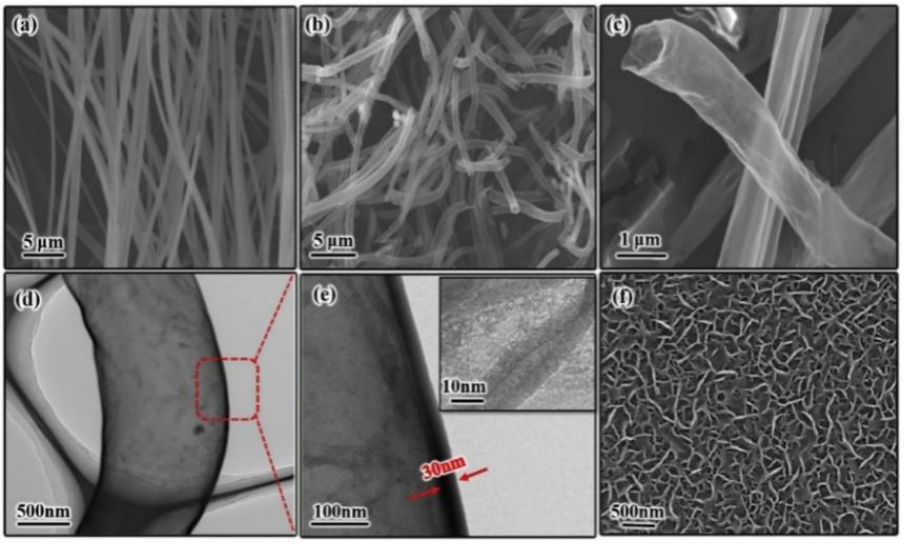

Figure 34. SEM images of (a) Electrospinning cellulose acetate fibers. For porous hollow SiO_2 nanotube, SEM images with (b) Low magnification and (c) high magnification, and TEM images with (d)Low magnification and (e) high magnification. (f) The etched glass substrate. Image adapted from reference [59].

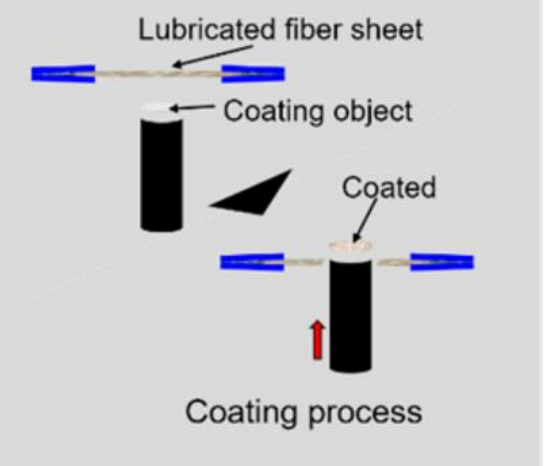

Figure 35. The lubricated fiber sheet sticks to the slippery surfaces and forms a coating on the endoscope lens. Image adapted from reference [57].

4. Conclusion

In this review, we have discussed natural and bio-inspired surfaces with anti-fouling properties. Defined as the settlement of undesired materials on the characters, fouling has numerous types and creates trouble for industrial applications. With wetting models and contact angle theories, mechanisms of many natural anti-fouling surfaces are studied, such as lotus leaves, shark skin, and pitcher plants. These mechanisms include low-contact hysteresis, hierarchical structures, and wettability. Artificial anti-fouling surfaces are usually designed by controlling surface chemistry to lower surface energy, modifying the microstructure on the characters, and changing their physical properties. The bio-inspired feelings show the same type of fouling resistance as the pristine nature surfaces, and some strategies can be applied in various areas. For example, superhydrophobic covers inspired by the lotus leaf show good anti-ice-fouling, anti-bio-fouling, and precipitation-fouling properties. Since natural surfaces usually have anti-fouling properties relating to their environment, exploiting more types of fouling resistance for one natural character is essential to work. On the other

hand, discovering an artificial surface that combines different fouling resistance and becomes omni-phobic is also a promising project.

Acknowledgment

Sanchuan Che, Muyi Ye, Yang Xie, Kayiu Li and Pengyou Du contributed equally to this work and should be considered co-first authors.

References

[1] Epstein, N. (1988). Particulate Fouling of Heat Transfer Surfaces: Mechanisms and Models. In: Melo, L.F., Bott, T.R., Bernardo, C.A. (eds) Fouling Science and Technology. NATO ASI Series, vol 145. Springer, Dordrecht. https://doi.org/10.1007/978-94-009-2813-8_10

[2] Fernandez-Torres, M. J., Fitzgerald, A. M., Paterson, W. R., & Wilson, D. I. (2001). A theoretical study of freezing fouling: limiting behaviour based on a heat and mass transfer analysis. Chemical Engineering and Processing: Process Intensification, 40(4), 335-344.

[3] Halvey, A. K., Macdonald, B., Dhyani, A., & Tuteja, A. (2019). Design of surfaces for controlling hard and soft fouling. Philosophical Transactions of the Royal Society A, 377(2138), 20180266.

[4] Petersen, Dennis S., et al. "Competing with barnacle cement: wetting resistance of a re-entrant surface reduces underwater adhesion of barnacles." Journal of The Royal Society Interface 15.145 (2018): 20180396.

[5] Huang, Yingfei, Zehua Wang, and Tom Chen. "Bio-Inspired Surfaces for Fouling Resistance." The Frontiers of Society, Science and Technology 2.10 (2020).

[6] Bhushan, Bharat. "Lessons from nature for green science and technology: an overview and bioinspired superliquiphobic/philic surfaces." Philosophical Transactions of the Royal Society A 377.2138 (2019): 20180274.

[7] Yeginbayeva, I. A., L. Granhag, and V. Chernoray. "A multi-aspect study of commercial coatings under the effect of surface roughness and fouling." Progress in Organic Coatings 135 (2019): 352-367.

[8] Xu, Yichun, Lixinhao Yang, and Haoran Zhang. "Bio-inspired Surfaces for Fouling Resistance, A Review." E3S Web of Conferences. Vol. 294. EDP Sciences, 2021.

[9] Ayyavoo, Jayalakshmi, et al. "Protection of polymeric membranes with antifouling surfacing via surface modifications." Colloids and Surfaces A: Physicochemical and Engineering Aspects 506 (2016): 190-201.

[10] Damodaran, V.B., Murthy, N.S. Bio-inspired strategies for designing antifouling biomaterials. Biomater Res 20, 18 (2016).

[11] Boase, Nathan RB, et al. "Polynitroxide copolymers to reduce biofilm fouling on surfaces." Polymer Chemistry 9.43 (2018): 5308-5318.

[12] Zhu, Ming-Ming, et al. "Antifouling and antibacterial behavior of membranes containing quaternary ammonium and zwitterionic polymers." Journal of Colloid and Interface Science 584 (2021): 225-235.

[13] Richards, Chloe, et al. "Bio-inspired surface texture modification as a viable feature of future aquatic antifouling strategies: a review." International Journal of Molecular Sciences 21.14 (2020): 5063.

[14] Keysar, S., et al. "Effect of surface roughness on the morphology of calcite crystallizing on mild steel." Journal of colloid and interface science 162.2 (1994): 311-319.

[15] Tong, Zheming, et al. "Squid inspired elastomer marine coating with efficient antifouling strategies: Hydrophilized defensive surface and lower modulus." Colloids and Surfaces B: Biointerfaces 213 (2022): 112392.

[16] Bixler, Gregory D., et al. "Anti-fouling properties of microstructured surfaces bio-inspired by rice leaves and butterfly wings." Journal of colloid and interface science 419 (2014): 114-133.

[17] Baum, C., Meyer, W., Roessner, D., Siebers, D., & Fleischer, L. G. (2001). A zymogel enhances the self-cleaning abilities of the skin of the pilot whale (Globicephala melas). Comparative Biochemistry and Physiology Part A: Molecular & Integrative Physiology, 130(4), 835-847.
[18] Amy, G. et al. (2017) 'Membrane-based seawater desalination: Present and future prospects', Desalination, 401, pp. 16–21. doi:10.1016/j.desal.2016.10.002.
[19] Bhushan, Bharat, and Yong Chae Jung. "Natural and biomimetic artificial surfaces for superhydrophobicity, self-cleaning, low adhesion, and drag reduction." Progress in Materials Science 56.1 (2011): 1-108.
[20] Camuffo, D. "Microclimate for Cultural Heritage-Conservation." Restoration, and Maintenance of Indoor and Outdoor Monuments (2014): 203-243.
[21] Jasper, Warren J., and Nadish Anand. "A generalized variational approach for predicting contact angles of sessile nano-droplets on both flat and curved surfaces." Journal of Molecular Liquids 281 (2019): 196-203.
[22] Jeevahan, J., Chandrasekaran, M., Britto Joseph, G., Durairaj, R. B., & Mageshwaran, G. J. J. O. C. T. (2018). Superhydrophobic surfaces: a review on fundamentals, applications, and challenges. Journal of Coatings Technology and Research, 15(2), 231-250.
[23] Falde, E. J., Yohe, S. T., Colson, Y. L., & Grinstaff, M. W. (2016). Superhydrophobic materials for biomedical applications. Biomaterials, 104, 87-103.
[24] Fei, L., He, Z., LaCoste, J. D., Nguyen, T. H., & Sun, Y. (2020). A mini review on superhydrophobic and transparent surfaces. The Chemical Record, 20(11), 1257-1268.
[25] Butt, Hans-Jürgen, et al. "Contact angle hysteresis." Current Opinion in Colloid & Interface Science (2022): 101574.
[26] Xu, Q.; Zhang, W.; Dong, C.; Sreeprasad, T.S.; Xia, Z. Biomimetic self-cleaning surfaces: Synthesis, mechanism and applications. J. R. Soc. Interface 2016, 13, 20160300.
[27] Collins, Christopher M., and Md Safiuddin. "Lotus-Leaf-Inspired Biomimetic Coatings: Different Types, Key Properties, and Applications in Infrastructures." Infrastructures (Basel) 7.4 (2022): 46. Web.
[28] Su, Yewang et al. "Nature's Design of Hierarchical Superhydrophobic Surfaces of a Water Strider for Low Adhesion and Low-Energy Dissipation." Langmuir 26.24 (2010): 18926–18937. Web.
[29] Kreder, Michael J., et al. "Design of anti-icing surfaces: smooth, textured or slippery?." Nature Reviews Materials 1.1 (2016): 1-15.
[30] Xie, Q., Pan, J., Ma, C., & Zhang, G. (2019). Dynamic surface antifouling: mechanism and systems. Soft Matter, 15(6), 1087-1107
[31] Jiang, Rujian et al. "Lotus-Leaf-Inspired Hierarchical Structured Surface with Non-Fouling and Mechanical Bactericidal Performances." Chemical engineering journal (Lausanne, Switzerland : 1996) 398 (2020): 125609. Web.
[32] Irajizad, Peyman, Sina Nazifi, and Hadi Ghasemi. "Icephobic surfaces: Definition and figures of merit." Advances in colloid and interface science 269 (2019): 203-218.
[33] Cao, Liangliang et al. "Anti-Icing Superhydrophobic Coatings." Langmuir 25.21 (2009): 12444–12448. Web.
[34] Rajiv, S., S. Kumaran, and M. Sathish. "Long-term-durable Anti-icing Superhydrophobic Composite Coatings." Journal of applied polymer science 136.7 (2019): 47059–n/a. Web.
[35] Hou, Deyin et al. "Biomimetic Superhydrophobic Membrane for Membrane Distillation with Robust Wetting and Fouling Resistance." Journal of membrane science 599 (2020): 117708. Web.
[36] Henry, C., Minier, J. P., & Lefèvre, G. (2012). Towards a description of particulate fouling: From single particle deposition to clogging. Advances in colloid and interface science, 185, 34-76.
[37] Shao Jingjing et al. "Research on Biomimetic Antifouling of Shark Skin." Coating Industry

38.10(2008):4.
[38] Wang, D., Xu, J., Yang, J., & Zhou, S. (2020). Preparation and synergistic antifouling effect of self-renewable coatings containing quaternary ammonium-functionalized SiO2 nanoparticles. Journal of colloid and interface science, 563, 261-271.
[39] Tian, L., Yin, Y., Bing, W., & Jin, E. (2021). Antifouling technology trends in marine environmental protection. Journal of Bionic Engineering, 18(2), 239-263.
[40] Baum, C., Meyer, W., Stelzer, R., Fleischer, L. G., & Siebers, D. (2002). Average nanorough skin surface of the pilot whale (Globicephala melas, Delphinidae): considerations on the self-cleaning abilities based on nanoroughness. Marine Biology, 140(3), 653-657.
[41] Scardino, A. J., & de Nys, R. (2011). Mini review: biomimetic models and bioinspired surfaces for fouling control. Biofouling, 27(1), 73-86.
[42] Baum, C., Simon, F., Meyer, W., Fleischer, L. G., Siebers, D., Kacza, J., & Seeger, J. (2003). Surface properties of the skin of the pilot whale Globicephala melas. Biofouling, 19(S1), 181-186.
[43] Yin, X., & Yu, B. (2015). Antifouling self-cleaning surfaces. In Antifouling Surfaces and Materials (pp. 1-29). Springer, Berlin, Heidelberg.
[44] Kirschner, C. M., & Brennan, A. B. (2012). Bio-inspired antifouling strategies. Annual review of materials research, 42, 211-229.
[45] Kwon, S. H., Lee, I., Park, H., & Lee, S. G. (2020). Decomposition mechanisms of self-polishing copolymers for antifouling coating materials through first-principles approach. Progress in Organic Coatings, 138, 105406.
[46] Xu, G., Liu, P., Pranantyo, D., Neoh, K. G., & Kang, E. T. (2018). Dextran-and chitosan-based antifouling, antimicrobial adhesion, and self-polishing multilayer coatings from pH-responsive linkages-enabled layer-by-layer assembly. ACS Sustainable Chemistry & Engineering, 6(3), 3916-3926.
[47] Zhou, X., Xie, Q., Ma, C., Chen, Z., & Zhang, G. (2015). Inhibition of marine biofouling by use of degradable and hydrolyzable silyl acrylate copolymer. Industrial & Engineering Chemistry Research, 54(39), 9559-9565.
[48] Box, Finn, Chris Thorogood, and Jian Hui Guan. "Guided droplet transport on synthetic slippery surfaces inspired by a pitcher plant." Journal of the Royal Society Interface 16.158 (2019): 20190323.
[49] Hsu, Chiao-Peng, Yu-Min Lin, and Po-Yu Chen. "Hierarchical structure and multifunctional surface properties of carnivorous pitcher plants Nepenthes." Jom 67.4 (2015): 744-753.
[50] Wong, Tak-Sing, et al. "Bioinspired self-repairing slippery surfaces with pressure-stable omniphobicity." Nature 477.7365 (2011): 443-447.
[51] Latthe, Sanjay S., et al. "Recent developments in air-trapped superhydrophobic and liquid-infused slippery surfaces for anti-icing application." Progress in Organic Coatings 137 (2019): 105373.
[52] Wang, Nan, et al. "Design and fabrication of the lyophobic slippery surface and its application in anti-icing." The Journal of Physical Chemistry C 120.20 (2016): 11054-11059.
[53] Zhu, Lin, et al. "Ice-phobic coatings based on silicon-oil-infused polydimethylsiloxane." ACS applied materials & interfaces 5.10 (2013): 4053-4062.
[54] Zhang, Jialei, Changdong Gu, and Jiangping Tu. "Robust slippery coating with superior corrosion resistance and anti-icing performance for AZ31B Mg alloy protection." ACS applied materials & interfaces 9.12 (2017): 11247-11257.
[55] Wang, Peng, Dun Zhang, and Zhou Lu. "Slippery liquid-infused porous surface bio-inspired by pitcher plant for marine anti-biofouling application." Colloids and Surfaces B: Biointerfaces 136 (2015): 240-247.
[56] Liu, Cansen, et al. "Investigation of vulcanization fouling behavior of biomimetic liquid-infused slippery surfaces." Journal of Materials Science 56.29 (2021): 16290-16306.
[57] Tenjimbayashi, Mizuki, et al. "In situ formation of slippery-liquid-infused nanofibrous surface

DOI: 10.54254/2755-2721/7/20230409

for a transparent antifouling endoscope lens." ACS Biomaterials Science & Engineering 4.5 (2018): 1871-1879.

[58] Wang, Chenghong, and Zhiguang Guo. "A comparison between superhydrophobic surfaces (SHS) and slippery liquid-infused porous surfaces (SLIPS) in application." Nanoscale 12.44 (2020): 22398-22424.

[59] Zhang, Meiling, et al. "Highly transparent and robust slippery lubricant-infused porous surfaces with anti-icing and anti-fouling performances." Journal of Alloys and Compounds 803 (2019): 51-60. [18]